



The conifer-curve: fast prediction of hydraulic conductivity loss and vulnerability to cavitation

Sabine Rosner¹ · Daniel M. Johnson² · Klara Voggeneder¹ · Jean-Christophe Domec^{3,4}

Received: 31 January 2019 / Accepted: 23 July 2019
© The Author(s) 2019

Abstract

• **Key message** The relationship between relative water loss (RWL) and hydraulic conductivity loss (PLC) in sapwood is robust across conifer species. We provide an empirical model (*conifer-curve*) for predicting PLC from simple RWL measurements. The approach is regarded as a new relevant phenotyping tool for drought sensitivity and offers reliable and fast prediction of diurnal, seasonal, or drought-induced changes in PLC.

• **Context** For conifer species drought is one of the main climate risks related to loss of hydraulic capacity in sapwood inducing dieback or mortality. More frequently occurring drought waves call for fast and easily applicable methods to predict drought sensitivity.

• **Aims** We aimed at developing a fast and reliable method for determination of the percent loss of hydraulic conductivity (PLC) and eventually the drought sensitivity trait P_{50} , i.e., the water potential that causes 50% conductivity loss.

• **Methods** We measured the loss of water transport capacity, defined as the relative water loss (RWL) together with PLC in trunk wood, branches, and saplings of eight different conifer species. Air injection was used to induce specific water potentials.

• **Results** The relationship between RWL and PLC was robust across species, organs, and age classes. The equation established allows fast prediction of PLC from simple gravimetric measurements and thus post hoc calculation of P_{50} ($r^2 = 0.94$).

• **Conclusion** The approach is regarded as a relevant new phenotyping tool. Future potential applications are screening conifers for drought sensitivity and a fast interpretation of diurnal, seasonal, or drought-induced changes in xylem water content upon their impact on conductivity loss.

Keywords Conifers · Drought stress · Hydraulic capacitance · Phenotyping · Vulnerability to cavitation

Handling Editor: Cyrille B. K. Rathgeber

Contribution of the co-authors: SR, KV, JCD, and DMJ performed the hydraulic measurements. SR made the data analysis and wrote a first draft of the manuscript. JCD and DMJ edited subsequent versions of the manuscript.

This article is part of the topical collection on *Wood formation and tree adaptation to climate*

✉ Sabine Rosner
sabine.rosner@boku.ac.at

¹ Institute of Botany, University of Natural Resources and Life Sciences, Gregor Mendel Str. 33, 1180 Vienna, Austria

² Warnell School of Forestry and Natural Resources, University of Georgia, Athens, GA 30602, USA

³ Nicholas School of the Environment, Duke University, Durham, NC 27708, USA

⁴ Bordeaux Sciences Agro, UMR 1391 INRA-ISPA, 33175 Gradignan Cedex, France

1 Introduction

Conifers are among the most endangered plant groups regarding forest dieback related to drought (Solberg 2004; Hentschel et al. 2014; Allen et al. 2015; Mencuccini and Binks 2015; McDowell and Allan 2015; Rosner et al. 2018; Klein et al. 2019). According to the International Union for Conservation of Nature (IUCN Red List), 34% of the world's conifers species are threatened (IUCN 2019). Facing global change (IPCC 2013), we urgently need fast and reliable screening tools for predicting drought sensitivity of conifer species and provenances thereof (David-Schwartz et al. 2016, Voltas et al. 2018). Screening tools should be economical, require little labor, not be time-consuming, easy in application and - last but not least - applicable to conifers worldwide. Recently, Rosner et al. (2019) presented an approach where hydraulic conductivity loss of angiosperm and conifer sapwood could be predicted from simple water loss measurements. The empirical predicting models in this preceding study were however species-specific. In the present study, we

aimed at developing one single prediction curve that would be applicable for conifers with a wide range of natural occurrence. The idea for a conifer prediction model developed because the relationship between relative water loss and conductivity loss varied widely among angiosperm species; the curves of conifer species showed a quite stable relationship (Rosner et al. 2019). Research on this plant group was also continued because their wood structure allows quite short sample lengths and application of several methods to measure hydraulic vulnerability that exists so far (Cochard et al. 2013, Klein et al. 2018).

Hydraulic performance of (secondary) xylem under drought and its recovery from drought depends on (I) hydraulic vulnerability to embolism, expressed as, e.g., P_{50} (i.e., the water potential resulting in 50% conductivity loss), (II) hydraulic safety margins, which is the P_{50} in relation to the minimum water potential measured in the field (Tyree and Sperry 1988, Choat et al. 2012; Delzon and Cochard 2014; Choat et al. 2018), and on (III) the capability of refilling emptied tracheids, which is presumably related to the hydraulic capacitance (Johnson et al. 2012; McCulloh et al. 2014; Trifilò et al. 2015, Klein et al. 2018), or (IV) the potential to produce new xylem tissue (Magnani and Borghetti 1995; Cochard et al. 2001). Water storage capacitance is the amount of water released from a tissue due to a defined decline in water potential (Tyree and Yang 1990; Meinzer et al. 2003; Domec et al. 2006). In general, more knowledge exists about species or organ-specific P_{50} and the shape of vulnerability curves (Choat et al. 2012), i.e., the percent loss of conductivity (PLC) plotted against the water potential (Ψ) (Sperry and Tyree 1988), than about hydraulic capacitance (Trifilò et al. 2015). Capacitance can be expressed as the increase in the absolute mass of water lost from a sample of defined volume per unit Ψ change but also as the increasing relative water loss (RWL) per unit Ψ change. The RWL method allows the comparison of the samples differing in total water volume and wood density (Domec and Gartner 2001). Rosner et al. (2019) defined an additional capacitance parameter, the RWL at P_{50} , i.e., the RWL that results from 50% conductivity loss. RWL at P_{50} varies widely across angiosperm and conifer species and is negatively related to wood density, as found for other capacitance traits as well (Pratt et al. 2007; Scholz et al. 2007; McCulloh et al. 2014; Trifilò et al. 2015; Savi et al. 2017; Pratt and Jacobsen 2017).

The aim of this study was to confirm the quite stable relationship between PLC and RWL (Rosner et al. 2019) across conifers species originating from different ecosystems around the globe. Such an approach should not only result in a fast prediction of species-, organ-, or age class-specific hydraulic vulnerabilities but will also allow us to establish the amount water remaining in xylem at P_{50} and P_{88} (Ψ at 88% PLC). We tested mature and juvenile trunkwood as well as branches of eight different conifer species with a broad range of natural occurrence from extremely wet environments (*Taxodium distichum*) to quite dry environments (*Juniperus virginiana*). We thus expected a wide range in

P_{50} . Most of the species investigated are also of high economical importance (*Abies nordmanniana*, *Larix decidua*, *Picea abies*, *Pinus ponderosa*, *Pinus taeda*, *Pseudotsuga menziesii*) which further substantiates the need for fast and reliable screening tools for selecting appropriate provenances with a higher drought tolerance.

2 Material and methods

2.1 Plant material

Information on the origin of the plant material is provided in Table 1. Eight different conifer species were investigated, which comprised *Abies nordmanniana* ((Stev.) Spach), *Juniperus virginiana* L., *Larix decidua* Mill., *Picea abies* (L.) Karst., *Pinus ponderosa* P. Lawson and C. Lawson, *Pinus taeda* L., *Pseudotsuga menziesii* (Mirbel) Franco, and *Taxodium distichum* L. Rich.

2.2 Determination of conductivity loss and relative water loss

Either whole saplings or side branches (cut from larger supporting branches with a length varying from 0.5 to 1.5 m) were harvested in the morning and transported to the lab in black plastic bags containing wet towels. Internodes with a length of 200 mm were cut and debarked underwater. They were re-saturated under low vacuum for 24 h at 4 °C in filtered, distilled water (Hietz et al. 2008) with 0.005% Micropur (Katadyn Products, Wallisellen, Switzerland). Prior to hydraulic measurements, specimens were shortened to 130 mm and then re-cut several times with clean razor blades. Sapwood area hydraulic conductivity (K_s , $\text{cm}^2 \text{s}^{-1} \text{MPa}^{-1}$) was measured under a hydraulic pressure head of 5.4 kPa (540 mm water column) with distilled and filtered (0.22 μm) water containing 0.005% Micropur. The saturated weight (SW) was determined on a balance (resolution of 0.0001 g, Mettler-Toledo International Inc., Greifensee, Switzerland). Air overpressure was applied in a double-ended pressure chamber (PMS Instruments, Corvallis, OR, USA), thereafter the specimen was weighed again in order to determine the fresh weight (FW) at a given pressure application. The pressure in the chamber was gradually increased with steps of 0.5 MPa or 1.0 MPa. The duration of the pressure exposition was standardized to 1 min (Rosner et al. 2019). Hydraulic vulnerability curves of trunk wood samples were achieved with the methods described by Spicer and Gartner (1998) and Domec and Gartner (2001). Results on PLC and RWL at given pressure applications for *L. decidua* and *P. abies* came from existing datasets (Rosner et al. 2008, Rosner et al. 2019). Tangential and radial faces of 200-mm long wood beams with a transverse surface of 100 mm^2 were shortened on a band saw and thereafter re-cut several times with a

razor blade. Specimens were re-soaked as described above (Hietz et al. 2008). The final dimensions of the specimens were 6 mm (radial) × 6 mm (tangential) × 120 mm (longitudinal).

Samples were dried at 103 °C for 24 h (Rosner 2017) in order to determine the dry weight (DW) on a balance. The relative water loss (RWL) at Ψ was calculated as:

$$\text{RWL (\%)} = 100 * (1 - ((\text{FW} - \text{DW}) / (\text{SW} - \text{DW}))) \quad (1)$$

The correct determination of the SW is crucial because relating FW to a field in situ water content would obscure the relationship between RWL and PLC and would not allow correct projection of PLC (Rosner et al. 2019).

2.3 Sample numbers, data processing, and statistical analyses

Numbers of sampled trees, samples and datasets can be found in Table 1. The software SPSS™ 21.0 was used to carry out the data analyses. Normal distribution was tested with the Kolmogorov-Smirnov test. Relationships between traits were accepted as significant if the *P* value was < 0.05.

Sapwood area-specific hydraulic conductivity at a given Ψ was divided by the sapwood area-specific hydraulic conductivity at full saturation in order to calculate the percent loss of conductivity (PLC). PLC was plotted against the negative of the applied pressure (Ψ). For some species, organs or age classes only mean values for PLC and RWL at a given pressure application were available. Hydraulic vulnerability curves were fitted by an exponential sigmoidal equation (Pammenter and Vander Willigen 1998), and the P_{50} and P_{88} (Domec and Gartner 2001), i.e., the pressure application at which 50% or 88% of conductivity loss occurred, were calculated. We used the following equation:

$$\text{PLC (\%)} = 100 / (1 + \exp(a * (\Psi - b))) \quad (2)$$

The parameter “*a*” corresponds to the slope of the linear part of the regression and “*b*” is the P_{50} . P_{88} was calculated from these parameters. Ψ in Eq. (2) is used here and thereafter for water potential. In Table 2, results for “*a*” and P_{50} are provided with their standard error and the 95% confidence interval (CI 95%).

The relationship between point measurements and mean PLC and RWL were tested by the “curve estimation” function in SPSS™ 21.0, where linear, quadratic, or cubic regressions were chosen according to their predictive quality. The chosen equation was used to calculate RWL at P_{50} for each species, organ, or age class. In Table 3, the CI 95% and 95% individual prediction intervals (PI 95%) for RWL at P_{50} or RWL at P_{88} are provided. Species, organ, and age class-specific mean values of PLC (PLC_{pred}) and RWL were fitted by a Weibull equation (e.g., Lopez et al. 2005):

$$\text{PLC}_{\text{pred}} = 100 - (100 / (\exp((\text{RWL}/c)^{**d}))) \quad (3)$$

The parameter “*c*” corresponds to the mean RWL across all conifers investigated in the study that causes ~63% of PLC.

Water loss curves, i.e., the RWL plotted against Ψ (RWL- Ψ curve) were fitted by the “curve estimation” function in SPSS™ 21.0. The fittings with the highest predictive quality (r^2) and the most reliable shape were chosen. The “curve estimation” function was also used to establish the relationship between Ψ and RWL in order to predict Ψ at a given RWL, for instance the RWL at P_{50} or at P_{88} . In these curves, the Ψ was plotted against the RWL (Ψ -RWL curve, Table 4).

The predictive quality of the RWL for PLC at the species, organ and age class level was tested by calculating empirically modeled P_{50} parameters from the RWL at P_{50} and the relationship between Ψ and RWL (Ψ -RWL curve). The same procedure was performed for P_{88} . The predicted values of P_{50} and P_{88} are provided with their 95% CI and 95% PI (Table 4). By means of the Eq. [3], PLC was predicted from RWL point measurements (if available) and mean values (Table 1). Thereafter, P_{50} and P_{88} parameters (Table 5) were calculated using Eq. [2]. Modeled P_{50} and P_{88} were related to the corresponding traits from directly measured datasets. Linear regression analysis was performed to meet the 1:1 slope requirement. A flow chart of the two different approaches is shown in Fig. 1.

3 Results

Conifer species investigated varied widely in their vulnerability to cavitation (Fig. 2, Table 2). In saplings, *A. nordmanniana* had the lowest P_{50} (− 8.1 MPa) and *P. menziesii* grown in Austria had the highest P_{50} (− 5.0 MPa). In branches, P_{50} ranged from − 5.8 MPa in *P. menziesii* to − 2.4 MPa in *T. distichum*. In general, P_{50} was highest in the wood of the main trunk, ranging from − 4.9 MPa in *P. menziesii* to − 2.2 MPa in *P. abies*. The species investigated varied as well in their RWL at a given pressure application (Fig. 2). For instance, whereas RWL increased only slightly with each pressure application in *A. nordmanniana* saplings (Fig. 2b), RWL had large increases over narrower pressure ranges in *P. abies* trunk wood (Fig. 2d).

PLC was strongly related to RWL at the species/organ/age-specific level (Table 3). Mean species/organ/age-specific PLC for a given Ψ and PLC predicted from the corresponding RWL dataset (Table 3) were therefore strongly linearly related (Fig. 3b). The RWL at P_{50} had values ranging from 15% in *L. decidua* saplings to 36% in *J. virginiana* trunk wood. By means of the species/organ/age-specific RWL at P_{50} and the relationship between Ψ and RWL (Table 4), P_{50} values could be predicted which correlated strongly (almost 1:1) with those calculated from the measured dataset (Fig. 4a). Predicted P_{88} was

as well strongly related to P_{88} derived from measured datasets ($r^2 = 0.98$, $P < 0.0001$).

In order to guarantee equal weight of each species-, organ-, and age class-specific PLC-RWL relationship, mean values for a given Ψ were used for the pooled data analysis (Fig. 3a). The relationship between PLC and RWL across all samples was fitted with the function:

$$PLC_{pred} = 100 - (100 / (\exp((RWL/30.49)**1.92))) \text{ (conifer-curve)} \quad (4)$$

PLC_{pred} is the predicted percent loss of hydraulic conductivity (Fig. 3c). More information on the parameters of Eq. (4) can be found in the legend of Fig. 3. RWL of 30.49% corresponds to a PLC_{pred} of ~63% across all conifer specimen investigated. RWL of 25.18% would then result in PLC_{pred} of 50%, and RWL of 45.12% would result in PLC_{pred} of 88% across species, organs, and age classes.

From RWL point measurements and the *conifer-curve*, PLC_{pred} values were calculated. PLC_{pred} values and the corresponding Ψ , was used to project P_{50} (Table 5). The correlation between P_{50} and the empirically modeled P_{50} (P_{50pred}) was tight ($r^2 = 0.94$, $P < 0.0001$), but no 1:1 relationship could be reached for specimens with low P_{50} (Fig. 6, in the Annex). A linear regression was therefore used for reliably predicting P_{50} (Fig. 4b).

$$P_{50pred'} = -0.75 + 0.82 * P_{50pred} \quad (r^2 = 0.97, P < 0.0001) \quad (5)$$

where $P_{50pred'}$ corresponds to P_{50pred} after slope correction. P_{88pred} was as well strongly related to P_{88} calculated from measured data ($r^2 = 0.98$, $P < 0.0001$).

Conifer species, organs or age classes with higher RWL at P_{50} or P_{88} were more vulnerable to cavitation: The positive relationship with P_{50} was however much stronger with RWL at P_{88} (Fig. 5). P_{88} showed as well an increase with increasing RWL at P_{88} ($r^2 = 0.44$, $P < 0.01$).

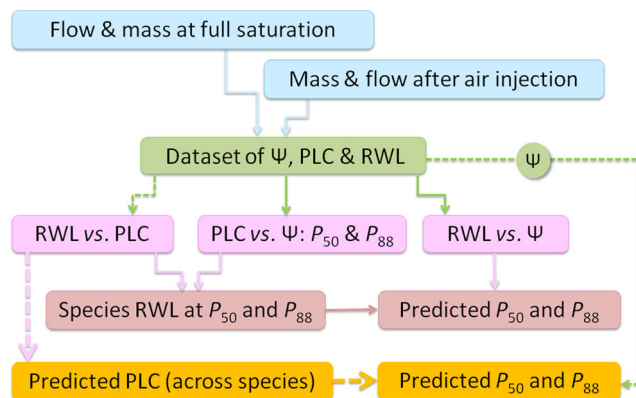


Fig. 1 Flow chart of the measuring procedure for the two model approaches for calculating the P_{50} or P_{88} . Hatched lines indicate the modeling procedure for the “conifer curve”, solid lines for the species-specific modeling approach to predict P_{50} or P_{88} . The dataset comprised the water potential (Ψ), the RWL (relative water loss) and the PLC (percent loss of conductivity)

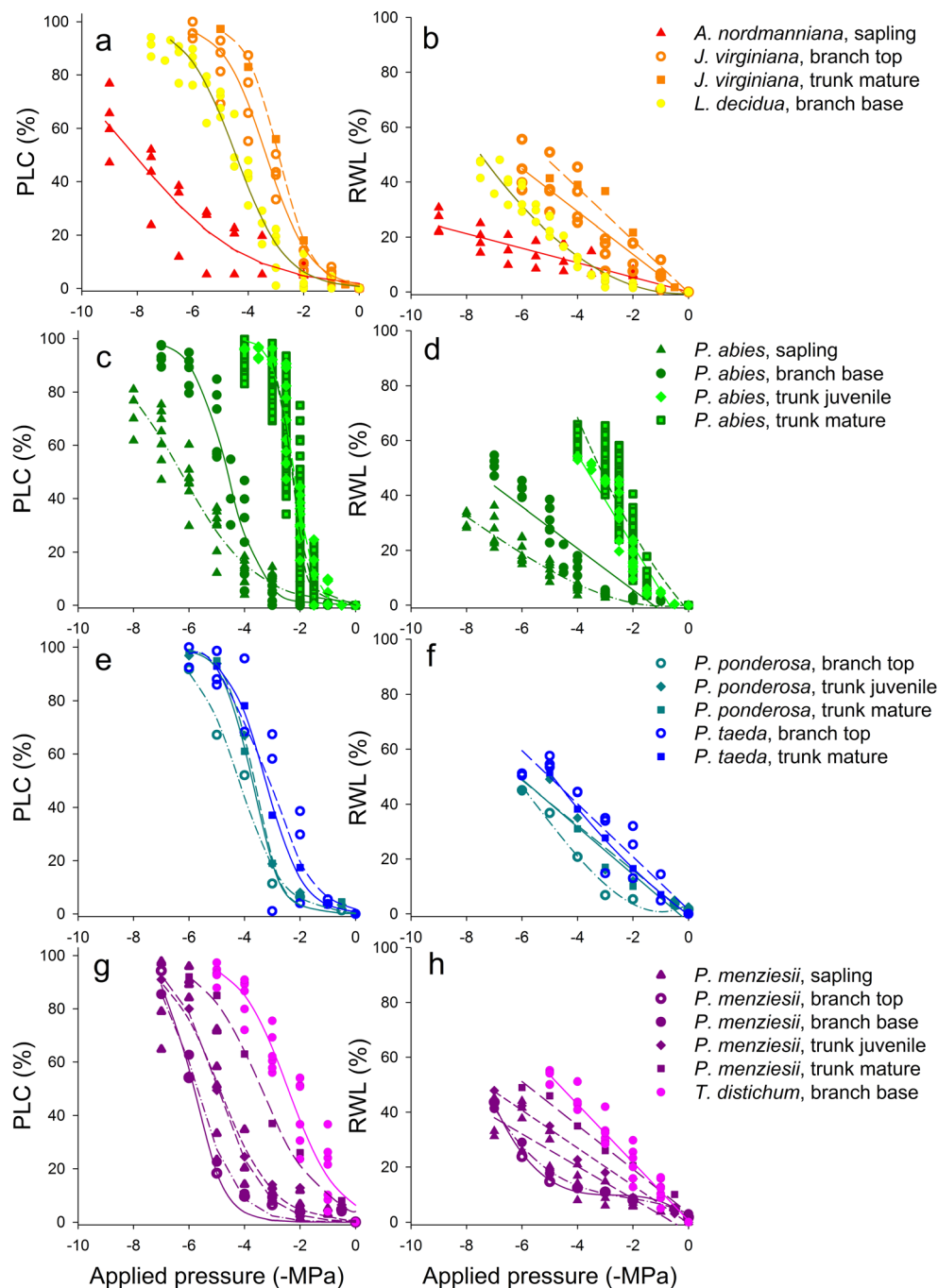
4 Discussion

This study tested whether an empirical relationship between the loss of water transport capacity and the loss of water content could be established across temperate conifer species. We found that it was possible to predict conductivity loss and eventually P_{50} or P_{88} for different conifer species, organs, and age classes with a coefficient of determination of 94% from quite simple RWL and Ψ measurements using one empirical model (*conifer-curve*, Fig. 3a). Although the RWL curves and the vulnerability curves differed widely between species, organs, or age classes (Fig. 2), the relationship between RWL and PLC is presumably quite conservative (Fig. 3). We discuss why this may be the case in conifers but not in angiosperms (Rosner et al. 2019), explore the relationship between hydraulic capacitance and vulnerability to cavitation, and propose how the technique could be further developed as a fast and reliable phenotyping tool.

4.1 Why is the relationship between RWL and PLC so robust?

Conifer wood is quite homogeneously constructed and solely one-cell type, the tracheid, fulfills the different functions of water transport and mechanical support (Braun 1970; Lachenbruch and McCulloh 2014). Species, organ, or age class-specific variability in late wood percent, lumen diameter, cell wall thickness, tracheid length, and pit properties result in different hydraulic vulnerabilities and water release curves (Domec and Gartner 2001; Hacke et al. 2001; Domec et al. 2009; Bouche et al. 2014; Hacke et al. 2015). We found a wide range in P_{50} values in the current study. In that regard, it was remarkable how the young trunk of *A. nordmanniana* saplings, with P_{50} of -8.1 MPa and trunk wood from the upper crown of mature *P. abies* trees with P_{50} of -2.2 MPa (Fig. 4) could be fitted into one PLC-RWL curve (*conifer-curve*, Fig. 3a) from which the species- and age class-specific PLC at a given Ψ could be reliably predicted from RWL data. This suggests that wood design in conifers is quite conservative concerning the PLC-RWL relationships. However, even if a given RWL results in a quite similar conductivity loss across different cambial age, anatomy can be adjusted to the hydraulic safety demands that are necessary for tree survival. The distance from the apex/tip influences tracheid size; tracheid lumen diameters are thus much smaller in saplings than at the lower trunk of mature trees of a given species (Anfodillo et al. 2013; Rosner 2017; Prendin et al. 2018); therefore, a stable PLC-RWL relationship suggests shorter tracheids and smaller pit aperture diameters with a higher torus overlap in saplings, which could additionally increase the hydraulic safety (Rosner 2013; Bouche et al. 2014; Hacke et al. 2015). Extreme shifts from the species mean PLC-RWL curve may come from the presence of

Fig. 2 Point measurements of percent loss of hydraulic conductivity (PLC) and the estimated vulnerability curves described in Table 2 in the Annex (a, c, e, g) and of relative water loss (RWL) and the estimated water loss curves described in Table 4 in the Annex (b, d, f, h) plotted against the water potential for different conifer species, organs or age classes



reaction wood. Compression wood (Fig. 7, in the Annex) has a high wood density, lower conductivity (Spicer and Gartner 1998), but is more vulnerable to cavitation than opposite wood (Mayr and Cochard 2003). For instance, *L. decidua* branches had a higher conductivity loss at given relative water loss compared with other species (Fig. 3a). RWL at P_{50} was only 15.1%. PLC in *L. decidua* predicted for a given Ψ with the *conifer-curve* was lower than the measured PLC (Fig. 3c). Therefore, P_{50} was lower (more negative) than the P_{50} calculated from predicted PLC values of the species-specific *L. decidua* curves (Fig. 4).

Such shifts in the PLC-RWL curves result in different hydraulic capacities, thus in differences between RWL at P_{50} or P_{88} .

4.2 Relationship between hydraulic capacitance and vulnerability to cavitation

Although the relationship between PLC and RWL is more stable in conifers than across angiosperm species (Rosner et al. 2019), species-, organ-, and age class-specific differences in the RWL at P_{50} do exist (Fig. 5). The RWL at P_{50}

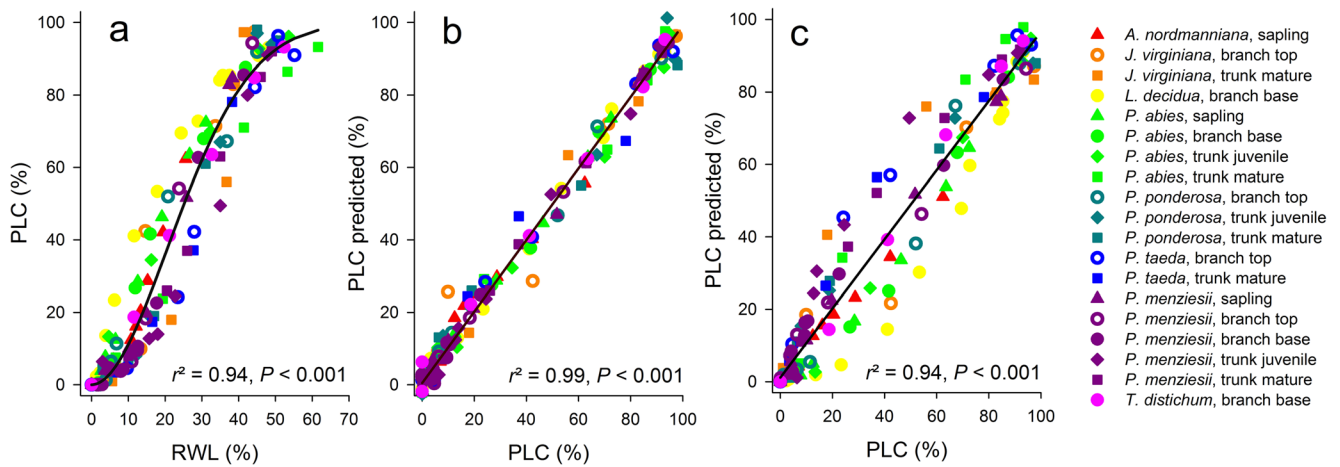


Fig. 3 Relationship between mean measured PLC and RWL across conifer species, organs and age classes for a given pressure application (Ψ): the “conifer-curve” (a), predicted mean PLC using species, organ and age specific curves (Table 3 in the Annex) (b) and predicted mean PLC using the “conifer-curve” (c) related both to mean measured PLC

values at a given Ψ . The equation in plot (a) is as follows: $PLC_{pred} = 100 - (100 / (\exp((RWL/c)^{**d})))$, where c is 30.49 ± 0.52 , 95% CI (29.46 31.52) and d is 1.92 ± 0.08 , 95% CI (1.75 2.08). Dataset number for all three plots is $n = 147$

can be regarded as a capacitance parameter (Rosner et al. 2019), which is very useful for comparing different species because no absolute values are used (Domec and Gartner 2001). We found a positive trend between P_{50} and the RWL at P_{50} and a significant positive relationship between P_{50} and RWL at P_{88} (Fig. 5). Similarly, McCulloh et al. (2014) found that mature conifer trunks had greater hydraulic vulnerability together with higher hydraulic capacitance than branches of the same species. Angiosperm branches with higher hydraulic capacitance also show less negative (higher) mean daily minimum water potentials (Meinzer et al. 2003). Species with higher P_{50} may therefore have more pronounced diurnal changes in conductivity loss (Trifilò et al. 2015). Within a plant, woody parts with higher hydraulic vulnerability but higher hydraulic capacitance may act as important storage compartments for water (Holbrook 1995). We have no sound

explanation why a stronger relationship existed between P_{50} and RWL at P_{88} than between P_{50} and RWL at P_{50} , because in conifers, P_{50} is regarded as a “point of no return” for the recovery from drought (Choat et al. 2018), even though some species can survive much lower conductivity losses (e.g., Hammond et al. 2019). It might be that the presence of reaction wood (Mayr and Cochard 2003) masks the relationship at high Ψ . The presence of reaction wood but also the distance from the apex/tip (Anfodillo et al. 2013; Rosner 2017; Prendin et al. 2018) may explain some different P_{50} values than those found in literature. Branch P_{50} values for *L. decidua*, *P. abies*, *P. ponderosa*, *P. taeda*, and *T. distichum* corresponded to those published earlier (reviewed in Choat et al. 2012, Bouche et al. 2014). We found however much higher (less negative) P_{50} for *J. virginiana* branches but slightly lower P_{50} in *P. menziesii* branches (reviewed in Choat et al. 2012).

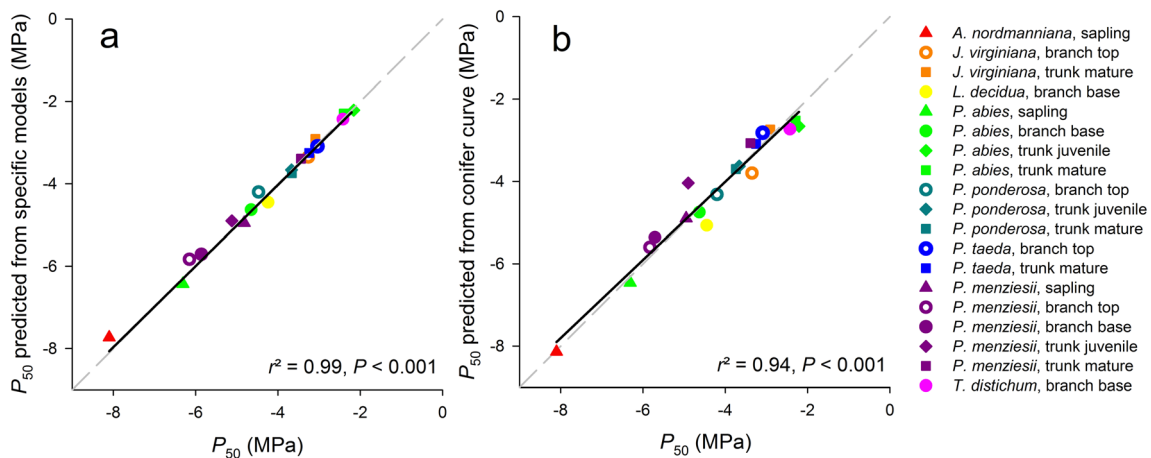


Fig. 4 Predicted pressure application that is necessary to result in 50% conductivity loss (P_{50}) from species/organ/age specific models (Tables 2, 3, and 4 in the Annex) (a) and P_{50} calculated from PLC predicted with the conifer-curve (eq. [4]) after slope correction (b) related to P_{50} derived

from experimental datasets. The slope correction (eq. [5]) was necessary because there was no 1:1 correlation (gray dashed lines) at lower P_{50} values (Fig. 6 in the Annex)

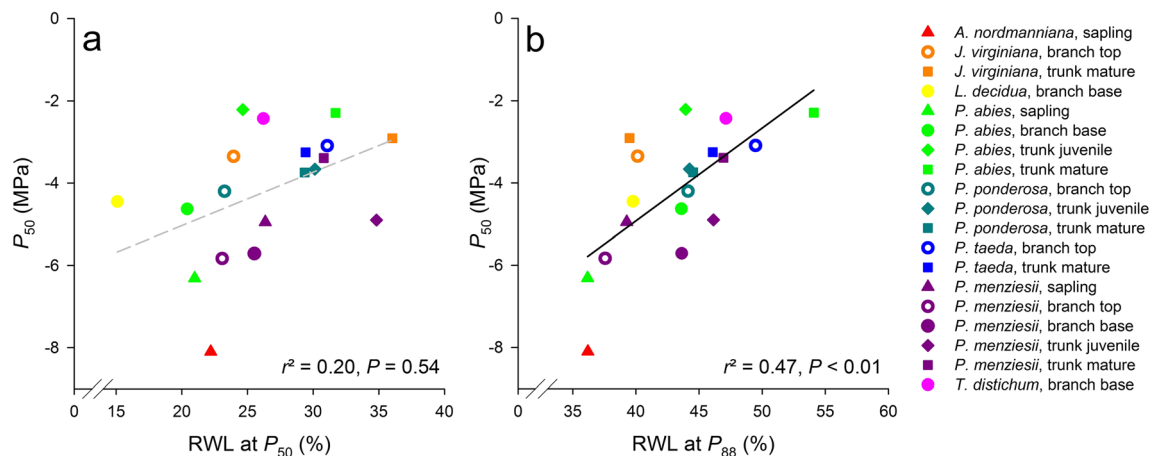


Fig. 5 Relationship between positive pressure that is necessary to result in 50% conductivity loss (P_{50}) and the RWL at P_{50} (a) and at P_{88} (b) for different conifer species, organs and age classes

4.3 Phenotyping: limits of application and further development of the method

Note that the empirical models for predicting PLC from RWL measurements and eventually P_{50} are applicable to functioning sapwood solely. In that regard, and except in Douglas-fir, the advantage of conifer wood is that many annual rings are used for conducting water (Bertaud and Holmbom 2004). However, reliable, standardized, sampling may be easier for wood of the main trunk than for small branches and shoots because the sapwood zone is easier to detect, and reaction wood can be avoided. However, when trunkwood is sampled, the distance from the apex/tip has to be considered (Anfodillo et al. 2013; Prendin et al. 2018). Even though branches used in general for vulnerability curves have a small diameter, they may be quite old (Schweingruber et al. 2008), and not all annual rings will necessarily transport water. It is thus important to harvest branches where the woody part consists of sapwood solely, which can be easily tested by staining techniques (Hietz et al. 2008). Moreover, we suggest performing experiments only during the growing season because (1) the bark is easier to remove from the woody parts, and (2) wood of temperate species harvested during the winter time shows a poorer ability to refill artificially, presumably because of natural pit aspiration (Mayr et al. 2014). The reliable prediction of the weight at full saturation is of utmost importance for the proposed technique, as already pointed out in a preceding study (Rosner et al. 2019). In a specimen that contains heartwood, the tracheids will not refill properly because many pits are permanently aspirated. Dehydration behavior of such “oversaturated” regions, i.e., artificially refilled regions that did not contribute to the sapflow in the living tree anymore (Pivovarov et al. 2016), might be different. Moreover, the application of positive pressure may result in water loss but not necessarily to a loss in hydraulic conductivity.

The method presented is much less labor intensive than repeated flow measurements and less prone to errors resulting from tracheids clogged with resin or other organic substances.

Nevertheless, the procedure could still be improved, regarding the time that was necessary to measure one specimen. It should be possible to collect the xylem sap that is released due to the pressure application in pre-weighed vials (Ennajeh et al. 2011; Savi et al. 2019) and calculate the fresh weight at a given Ψ from subtracting the mass of water. A whole vulnerability curve could thus be produced within less than a quarter of an hour. Consensus should be about the time of pressure application and the pre-preparation of the specimens (Mayr et al. 2006), because this can influence the relationship between the RWL and Ψ . The method of stress application that leads to conductivity loss (e.g., bench top dehydration, pressure collar) has no influence on the relationship between RWL and PLC (Rosner et al. 2019), but for predicting P_{50} , Ψ -RWL datasets are necessary, which simulate the situation in the living tree. In that regard, it is likely that the *conifer-curve* is not applicable for RWL datasets of very small wood samples where Ψ is measured in a small chamber of a thermocouple psychrometer (Meinzer et al. 2003; Barnard et al. 2011; McCulloh et al. 2014; Jupa et al. 2016; Pratt and Jacobsen 2017), because the curve shapes often differ from those measured on bigger samples (Domec and Gartner 2001, 2002; Domec et al. 2006; Gleason et al. 2014; Blackman et al. 2016). Due to the high amount of cut open surfaces in relation to volume, dehydration in small wood samples will proceed quite fast and probably not from the more vulnerable to the less vulnerable tracheids but from the outside to the inside of the specimen (Rosner et al. 2019).

5 Conclusions

We were able to construct one empirical model equation in order to predict conductivity loss and eventually P_{50} for different conifer species originating from different ecosystems. The method offers fast and reliable prediction of PLC from quite simple and fast RWL and Ψ measurements and could be thus applied as an efficient phenotyping tool for P_{50} . Future research should test this PLC-RWL in conifer species not included in this study to

determine if the relationship is universal. The knowledge of this relationship can help interpret decent indirect anatomy-based techniques such as X-ray micro-computed tomography or neutron radiography. Future potential applications of the new method presented are screening trees for drought sensitivity and a fast interpretation of diurnal, seasonal, or drought-induced changes in xylem water content upon their impact on conductivity loss.

Acknowledgements We thank Helga Amreiter (Pötzleinsdorfer Schlosspark, Vienna, MA 42) for providing plant material of *Taxodium distichum*.

Statement on data availability The dataset for the “conifer-curve” is available from the corresponding author on reasonable request.

Funding Information Open access funding provided by University of Natural Resources and Life Sciences Vienna (BOKU). This study has received funding from the European Union’s Horizon 2020 research and innovation program under the Marie Skłodowska-Curie grant agreement No 645654 (Topwood). DMJ was partially supported by NSF IOS-

165731 and JCD and DMJ were partially supported by NSF IOS-1754893.

Compliance with ethical standards

Conflict of interest The authors declare that they have no conflict of interest.

Abbreviations CI 95%, 95% confidence intervals; DW, dry weight; FW, fresh weight; P_{50} , positive pressure resulting in 50% conductivity loss; P_{50pred} , positive pressure resulting in 50% conductivity loss calculated from PLC_{pred} ; P_{50pred} , P_{50pred} after slope correction; P_{88} , positive pressure resulting in 88% conductivity loss; P_{88pred} , positive pressure resulting in 88% conductivity loss calculated from PLC_{pred} ; PI 95%, 95% individual prediction intervals; PLC, percent loss of conductivity; PLC_{pred} , PLC predicted from RWL; RWL, relative water loss; RWL at P_{50} , RWL at Ψ when 50% conductivity is lost; RWL at P_{88} , RWL at Ψ when 88% conductivity is lost; SW, water-saturated weight; Ψ , xylem pressure

Annex

Table 1 Information on the origin of the plant material, on the age of the trees (age), the amount of tree individuals investigated (tree), the sample numbers (sample) as well as the dataset numbers (data, i.e., single hydraulic measurements)

Species	Origin	Lat.	Long.	Alt. [m]	Age	Tree	Organ	Sample	Data
<i>Abies nordmanniana</i>	Botanical garden, Vienna, Austria	48° 14' 12"	16° 20' 15"	233	4	3	Sapling	4	27
<i>Juniperus virginiana</i>	Duke Forest, Durham, NC, USA	35° 97' 82"	-79° 09' 42"	127	18	4	Branch top	4	28
<i>Juniperus virginiana</i>	Duke Forest, Durham, NC, USA	35° 97' 82"	-79° 09' 42"	127	18	6	Trunk mature	6	7*
<i>Larix decidua</i>	Botanical garden, Vienna, Austria	48° 14' 12"	16° 20' 15"	233	20	2	Branch base	8	52
<i>Picea abies</i>	Botanical garden, Vienna, Austria	48° 14' 12"	16° 20' 15"	233	4	8	Sapling	8	54
<i>Picea abies</i>	Botanical garden, Vienna, Austria	48° 14' 12"	16° 20' 15"	233	20	5	Branch base	6	46
<i>Picea abies</i>	Sande, Southern Norway	59° 34' 50"	10° 16' 29"	105	40	6	Trunk juvenile	18	44
<i>Picea abies</i>	Tönnersjöheden/Vissefjärda, Sweden	56° 67' 56" 54'	13° 07' 15" 53'	60/120	24	44	Trunk mature	95	428
<i>Pinus ponderosa</i>	Oregon Cascade Range, Gilchrist, OR, USA	43° 32' 25"	-121° 59' 38"	1355	225	6	Branch top	6	7*
<i>Pinus ponderosa</i>	Oregon Cascade Range, Gilchrist, OR, USA	43° 32' 25"	-121° 59' 38"	1355	225	6	Trunk juvenile	6	7*
<i>Pinus ponderosa</i>	Oregon Cascade Range, Gilchrist, OR, USA	43° 32' 25"	-121° 59' 38"	1355	225	6	Trunk mature	6	7*
<i>Pinus taeda</i>	Duke Face experimental site, Chapel Hill, NC, USA	35° 58' 39"	-79° 08' 18"	61	26	3	Branch top	3	18
<i>Pinus taeda</i>	Duke Face experimental site, Chapel Hill, NC, USA	35° 58' 39"	-79° 08' 18"	61	26	6	Trunk mature	6	6*
<i>Pseudotsuga menziesii</i>	Botanical garden, Vienna, Austria	48° 14' 12"	16° 20' 15"	233	4	6	Sapling	6	36
<i>Pseudotsuga menziesii</i>	Oregon Coast Range, Riddle, OR, USA	42° 57' 52"	-123° 21' 76"	220	116	6	Branch top	6	8*
<i>Pseudotsuga menziesii</i>	Oregon Coast Range, Riddle, OR, USA	42° 57' 52"	-123° 21' 76"	220	116	6	Branch base	6	8*
<i>Pseudotsuga menziesii</i>	Oregon Coast Range, Riddle, OR, USA	42° 57' 52"	-123° 21' 76"	220	116	6	Trunk juvenile	6	8*
<i>Pseudotsuga menziesii</i>	Oregon Coast Range, Riddle, OR, USA	42° 57' 52"	-123° 21' 76"	220	116	6	Trunk mature	6	8*
<i>Taxodium distichum</i>	Pötzleinsdorfer Schlosspark, Vienna, Austria	48° 14' 33"	16° 18' 21"	233	20	3	Branch base	7	39

Branches came either from the base of the crown (branch base) or from its top (branch top). Datasets are marked with *where only mean value datasets were available

Table 2 Information on the hydraulic vulnerability curves fitted by an exponential sigmoidal equation (percent loss of conductivity = $100/(1 + \exp.(a*(\text{pressure}-b)))$) (Pammenter and VanderWilligen 1998)

Species	<i>a</i>	<i>P</i> ₅₀ (MPa)	<i>r</i> ²	<i>P</i>	<i>P</i> ₈₈ (MPa)
<i>Abies nordmanniana</i> sapling	0.49 ± 0.07	-8.10 ± 0.25 (-8.61 -7.59)	0.84	<0.0001	-12.14
<i>Juniperus virginiana</i> branch, top of canopy	1.26 ± 0.12	-3.35 ± 0.08 (-3.52 -3.19)	0.96	<0.0001	-4.93
<i>Juniperus virginiana</i> trunk mature	1.65 ± 0.10	-2.91 ± 0.04 (-3.01 -2.80)	0.99	<0.0001	-4.11
<i>Larix decidua</i> branch, base of canopy	1.11 ± 0.06	-4.45 ± 0.05 (-4.55 -4.34)	0.97	<0.0001	-6.24
<i>Picea abies</i> sapling	0.74 ± 0.05	-6.31 ± 0.08 (-6.46 -6.15)	0.93	<0.0001	-9.01
<i>Picea abies</i> branch, base of canopy	1.62 ± 0.15	-4.63 ± 0.06 (-4.74 -4.51)	0.96	<0.0001	-5.85
<i>Picea abies</i> trunk juvenile	2.86 ± 0.27	-2.21 ± 0.03 (-2.27 -2.15)	0.94	<0.0001	-2.91
<i>Picea abies</i> trunk mature	3.44 ± 0.13	-2.29 ± 0.01 (-2.32 -2.27)	0.93	<0.0001	-2.87
<i>Pinus ponderosa</i> branch, top of canopy	1.25 ± 0.18	-4.20 ± 0.12 (-4.51 -3.89)	0.98	<0.0001	-5.79
<i>Pinus ponderosa</i> trunk juvenile	2.01 ± 0.17	-3.67 ± 0.05 (-3.79 -3.54)	0.99	<0.0001	-4.66
<i>Pinus ponderosa</i> trunk mature	1.94 ± 0.16	-3.74 ± 0.05 (-3.87 -3.61)	0.99	<0.0001	-4.77
<i>Pinus taeda</i> branch, top of canopy	1.29 ± 0.31	-3.09 ± 0.21 (-3.53 -2.65)	0.86	<0.0001	-4.64
<i>Pinus taeda</i> trunk mature	1.50 ± 0.12	-3.25 ± 0.06 (-3.42 -3.08)	0.99	<0.0001	-4.58
<i>Pseudotsuga menziesii</i> sapling	1.24 ± 0.17	-4.95 ± 0.11 (-5.18 -4.72)	0.90	<0.0001	-6.56
<i>Pseudotsuga menziesii</i> branch, top of canopy	1.79 ± 0.26	-5.83 ± 0.10 (-6.05 -5.62)	0.99	<0.0001	-6.95
<i>Pseudotsuga menziesii</i> branch, base of canopy	1.39 ± 0.16	-5.71 ± 0.09 (-5.92 -5.49)	0.99	<0.0001	-7.14
<i>Pseudotsuga menziesii</i> trunk juvenile	1.04 ± 0.12	-4.90 ± 0.12 (-5.19 -4.62)	0.99	<0.0001	-6.82
<i>Pseudotsuga menziesii</i> trunk mature	0.94 ± 0.08	-3.39 ± 0.09 (-3.63 -3.15)	0.99	<0.0001	-5.50
<i>Taxodium distichum</i> branch, base of canopy	1.11 ± 0.09	-2.43 ± 0.08 (-2.59 -2.27)	0.95	<0.0001	-4.32

The parameter “*a*” corresponds to the slope of the linear part of the regression and “*b*” is the *P*₅₀, i.e., the pressure that is necessary to result in 50% conductivity loss. *P*₈₈ is the pressure that would result in 88% conductivity loss (Domec and Gartner 2001). Results for *a* and *P*₅₀ are given with ± standard error and the 95% confidence interval (CI 95%) is given in brackets. Information on the sample and dataset numbers is given in Table 1

Table 3 Parameters for linear (b_0 , b_1), quadratic (b_0 , b_1 , b_2) or cubic (b_0 , b_1 , b_2 , b_3) equations for the relationship between percent loss of conductivity (PLC, independent variable) and the relative water loss (RWL, dependent variable) ($P < 0.0001$), the calculated RWL resulting in 50% (RWL at P_{50}) and 88% (RWL at P_{88}) of conductivity loss and their 95% confidence intervals (CI 95%) and 95% individual prediction intervals (PI 95%) for different conifer species and different age classes

Species and organ	b_0	b_1	b_2	b_3	r^2	RWL at P_{50} (CI 95%, PI 95%) (%)	RWL at P_{88} (CI 95%, PI 95%) (%)
<i>Abies nordmanniana</i> sapling	3.7756	0.3684			0.89	22.20 (20.37 24.02, 15.68 28.71)	36.19 (32.55 39.84, 28.96 43.43)
<i>Juniperus virginiana</i> branch, top of canopy	2.6466	0.4260			0.90	23.94 (21.76 26.13, 12.30 35.59)	40.13 (36.82 43.44, 28.22 52.04)
<i>Juniperus virginiana</i> trunk mature	1.2356	1.4675	-0.02030	9.735E-5	0.99	36.02 (33.37 38.62, 27.45 44.59)	39.49 (35.32 43.65, 31.42 47.55)
<i>Larix decidua</i> branch, base of canopy	1.3540	0.0617	0.00426		0.98	15.09 (14.46 15.71, 10.61 19.57)	39.77 (38.75 40.79, 35.28 44.26)
<i>Picea abies</i> sapling	0.9642	0.4001			0.94	20.97 (19.98 21.96, 15.41 26.54)	36.17 (34.26 38.09, 30.37 41.97)
<i>Picea abies</i> branch, base of canopy	1.7912	0.3703	-0.00147	3.028E-5	0.98	20.41 (19.60 21.21, 15.07 25.74)	43.60 (42.30 44.89, 38.31 48.88)
<i>Picea abies</i> trunk juvenile	-0.7449	0.5076			0.96	24.64 (23.55 25.72, 17.40 31.87)	43.93 (42.27 45.59, 36.58 51.27)
<i>Picea abies</i> trunk mature	2.2361	0.5892			0.96	31.70 (31.30 32.20, 22.27 41.13)	54.09 (54.53 55.82, 44.65 63.53)
<i>Pinus ponderosa</i> branch, top of canopy	3.5165	0.0531	0.009710	-5.761E-5	0.98	23.25 (18.86 27.65, 10.14 36.36)	44.13 (36.70 51.60, 30.60 57.65)
<i>Pinus ponderosa</i> trunk juvenile	4.2940	0.5992	-0.00165		0.99	30.13 (27.11 33.14, 19.32 40.93)	44.24 (39.71 48.76, 35.20 53.27)
<i>Pinus ponderosa</i> trunk mature	2.6332	0.6110	-0.00153		0.97	29.35 (24.81 33.90, 13.60 45.10)	44.54 (37.68 51.39, 30.93 58.14)
<i>Pinus taeda</i> branch, top of canopy	6.8426	0.4846			0.92	31.07 (27.99 34.15, 17.70 44.44)	49.48 (45.06 53.90, 35.74 63.23)
<i>Pinus taeda</i> trunk mature	0.9323	1.3476			0.99	29.42 (29.20 34.54, 17.80 41.03)	46.09 (38.90 56.30, 35.53 56.66)
<i>Pseudotsuga menziesii</i> sapling	2.8286	0.5447	-0.00148		0.95	26.35 (25.08 27.63, 18.99 33.71)	39.27 (34.13 41.40, 31.95 46.58)
<i>Pseudotsuga menziesii</i> branch, top of canopy	2.6957	1.0666	-0.02050	0.000146	0.99	23.07 (20.36 25.80, 15.09 31.06)	37.56 (32.80 42.31, 29.49 45.63)
<i>Pseudotsuga menziesii</i> branch, base of canopy	2.9799	1.0017	-0.01744	0.000128	0.99	25.52 (23.75 27.30, 20.27 30.78)	43.63 (40.45 46.80, 37.63 49.62)
<i>Pseudotsuga menziesii</i> trunk juvenile	-1.4968	1.4887	-0.02114	0.000118	0.99	34.82 (31.87 37.78, 25.05 44.60)	46.14 (41.01 51.28, 36.66 55.62)
<i>Pseudotsuga menziesii</i> trunk mature	0.8228	1.0821	-0.01399	8.696E-5	0.99	30.81 (29.38 32.23, 26.24 35.38)	46.93 (44.63 49.24, 42.44 51.42)
<i>Taxodium distichum</i> branch, base of canopy	1.1029	0.4746	0.00055		0.97	26.21 (25.03 27.39, 18.60 33.82)	47.13 (45.33 48.93, 39.55 54.71)

P is < 0.0001 for all equations listed

Table 4 Relationship between pressure application and the relative water loss (RWL, independent variable) for the prediction of P_{50}

Species and organ	b_0	b_1	b_2	b_3	r^2	P_{50pred} (95% CI, 95% PI) (MPa)	P_{88pred} (95% CI, 95% PI) (MPa)
<i>Abies nordmanniana</i> sapling	-0.8447	-0.3100			0.82	-7.73 (-8.48 -6.97, -10.50 -4.95)	-12.06 (-13.54 -10.59, -15.12 -9.01)
<i>Juniperus virginiana</i> branch, top of canopy	-0.6582	-0.1088			0.85	-3.26 (-3.58 -2.95, -4.96 -1.57)	-5.03 (-5.49 -4.56, -6.76 -3.30)
<i>Juniperus virginiana</i> trunk	0.0592	-0.3141	0.0169	-0.00029	0.99	-3.09 (-3.49 -2.70, -4.07 -2.11)	-4.13 (-4.57 -3.69, -5.03 -3.22)
<i>Larix decidua</i> branch, base of canopy	-1.0639	-0.2530	0.0028		0.91	-4.24 (-4.45 -4.04, -5.74 -2.74)	-6.68 (-7.05 -6.31, -8.19 -5.17)
<i>Picea abies</i> sapling	-0.4061	-0.6779	0.0266	-0.00040	0.95	-6.43 (-6.63 -6.22, -7.61 -5.24)	-8.15 (-8.54 -7.76, -9.54 -6.76)
<i>Picea abies</i> branch, base of canopy	-1.2307	-0.2109	0.0021		0.87	-4.65 (-4.89 -4.40, -6.35 -2.95)	-6.39 (-6.83 -5.98, -8.09 -4.70)
<i>Picea abies</i> trunk wood crown	-0.9150	-0.0505			0.83	-2.16 (-2.29 -2.03, -3.02 -1.30)	-3.13 (-3.33 -2.94, -4.00 -2.26)
<i>Picea abies</i> trunk wood mature	-0.3351	-0.0816	0.0005		0.88	-2.40 (-2.44 -2.36, -3.27 -1.54)	-3.24 (-3.30 -3.18, -4.11 -2.37)
<i>Pinus ponderosa</i> branch, top of canopy	0.9006	3.5165	0.0234	-0.00029	0.96	-4.47 (-5.31 -3.62, -7.18 -1.75)	-5.89 (-7.43 -4.36, -8.65 -3.13)
<i>Pinus ponderosa</i> trunk juvenile	-0.3019	-0.1118			0.92	-3.67 (-4.41 -2.93, -5.64 -1.70)	-5.25 (-6.31 -4.19, -7.36 -3.14)
<i>Pinus ponderosa</i> trunk mature	-0.5460	-0.1062			0.92	-3.66 (-4.39 -2.95, -5.60 -1.74)	-5.28 (-6.32 -4.23, -7.34 -3.21)
<i>Pinus taeda</i> branch, top of canopy	-0.1886	-0.0919			0.89	-3.04 (-3.39 -2.69, -4.57 -1.52)	-4.73 (-5.23 -4.24, -6.30 -3.17)
<i>Pinus taeda</i> trunk mature	-0.0690	-0.1238	0.0006		0.99	-3.24 (-3.35 -3.12, -3.55 -2.92)	-4.61 (-4.79 -4.44, -4.93 -4.29)
<i>Pseudotsuga menziesii</i> sapling	-1.0203	-0.1440			0.85	-4.82 (-5.17 -4.46, -6.70 -2.93)	-6.68 (-7.22 -6.13, -8.60 -4.75)
<i>Pseudotsuga menziesii</i> branch, top of canopy	1.2217	-0.5071	0.0091	-0.00004	0.98	-6.15 (-6.73 -5.57, -8.01 -4.29)	-7.17 (-8.18 -6.16, -9.38 -4.95)
<i>Pseudotsuga menziesii</i> branch, base of canopy	1.9733	-0.6419	0.0177	-0.00018	0.99	-5.86 (-6.24 -5.47 -6.99 -4.74)	-7.21 (-7.97 -6.46, -8.73 -5.69)
<i>Pseudotsuga menziesii</i> trunk juvenile	-0.1320	-0.1432			0.98	-5.12 (-5.48 -4.76, -6.02 -4.21)	-6.74 (-7.25 -6.23, -7.71 -5.76)
<i>Pseudotsuga menziesii</i> trunk mature	0.3430	-0.1228			0.98	-3.44 (-3.76 -3.12, -4.33 -2.55)	-5.42 (-5.91 -4.93, -6.38 -4.46)
<i>Taxodium distichum</i> branch, base of canopy	0.0498	-0.0905			0.96	-2.42 (-2.53 -2.31, -3.14 -1.70)	-4.32 (-4.49 -4.14, -5.05 -3.58)

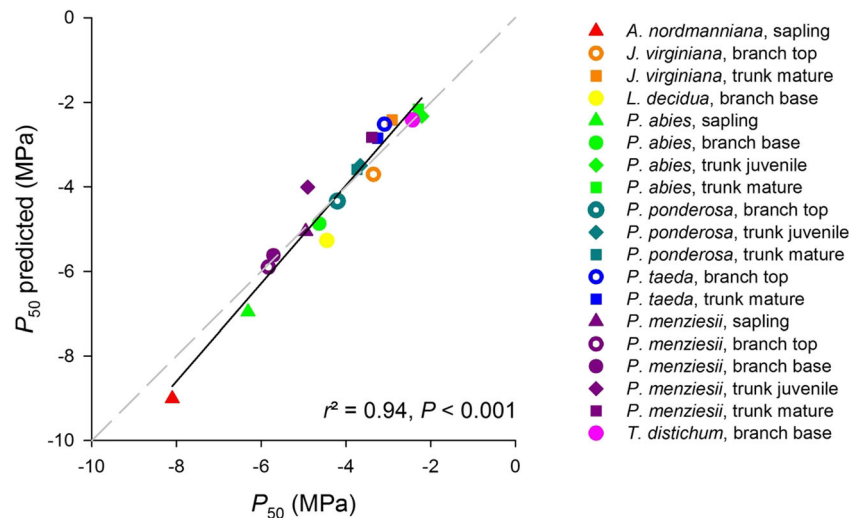
Equation parameters are given either for linear (b_0, b_1), quadratic (b_0, b_1, b_2), or cubic (b_0, b_1, b_2, b_3) equations for branches, saplings, or trunk wood of different conifer species. The predicted values of P_{50} and P_{88} are given with their 95% confidence intervals (95% CI) and 95% prediction intervals (95% PI). P is < 0.0001 for all equations listed

Table 5 Information on the hydraulic vulnerability curves fitted by an exponential sigmoidal equation (percent loss of conductivity = $100/(1 + \exp.(a*(\text{pressure}-b)))$) (Pammenter and VanderWilligen 1998)

Species	a	$P_{50\text{pred}}$ (MPa)	r^2	P	$P_{88\text{pred}}$ (MPa)
<i>Abies nordmanniana</i> sapling	0.41 ± 0.06	-9.01 ± 0.37 (-9.78 –8.24)	0.78	< 0.0001	-13.92
<i>Juniperus virginiana</i> branch, top of canopy	1.01 ± 0.14	-3.71 ± 0.15 (-4.02 –3.41)	0.89	< 0.0001	-5.68
<i>Juniperus virginiana</i> trunk mature	1.42 ± 0.10	-2.42 ± 0.20 (-2.93 –1.90)	0.97	< 0.0001	-3.82
<i>Larix decidua</i> branch, base of canopy	1.22 ± 0.07	-5.27 ± 0.05 (-5.37 –5.16)	0.97	< 0.0001	-6.90
<i>Picea abies</i> sapling	0.81 ± 0.06	-6.96 ± 0.09 (-7.14 –6.77)	0.91	< 0.0001	-9.42
<i>Picea abies</i> branch, base of canopy	1.84 ± 0.17	-4.87 ± 0.05 (-4.97 –4.76)	0.96	< 0.0001	-5.95
<i>Picea abies</i> trunk juvenile	3.18 ± 0.37	-2.33 ± 0.04 (-2.40 –2.25)	0.92	< 0.0001	-2.95
<i>Picea abies</i> trunk mature	4.10 ± 0.13	-2.16 ± 0.01 (-2.17 –2.14)	0.93	< 0.0001	-2.64
<i>Pinus ponderosa</i> branch, top of canopy	1.63 ± 0.16	-4.34 ± 0.07 (-4.52 –4.16)	0.99	< 0.0001	-5.57
<i>Pinus ponderosa</i> trunk juvenile	1.51 ± 0.26	-3.50 ± 0.13 (-3.83 –3.17)	0.98	< 0.0001	-4.82
<i>Pinus ponderosa</i> trunk mature	1.45 ± 0.18	-3.59 ± 0.10 (-3.84 –3.34)	0.99	< 0.0001	-4.97
<i>Pinus taeda</i> branch, top of canopy	1.09 ± 0.25	-2.52 ± 0.21 (-2.98 –2.07)	0.86	< 0.0001	-4.35
<i>Pinus taeda</i> trunk mature	1.27 ± 0.08	-2.85 ± 0.06 (-3.01 –2.70)	0.99	< 0.0001	-4.42
<i>Pseudotsuga menziesii</i> sapling	0.94 ± 0.11	-5.05 ± 0.12 (-5.30 –4.80)	0.89	< 0.0001	-7.16
<i>Pseudotsuga menziesii</i> branch, top of canopy	1.14 ± 0.22	-5.90 ± 0.17 (-6.32 –5.49)	0.96	< 0.0001	-7.66
<i>Pseudotsuga menziesii</i> branch, base of canopy	0.99 ± 0.11	-5.62 ± 0.11 (-5.89 –5.35)	0.99	< 0.0001	-7.63
<i>Pseudotsuga menziesii</i> trunk juvenile	0.81 ± 0.09	-4.01 ± 0.14 (-4.35 –3.67)	0.98	< 0.0001	-6.46
<i>Pseudotsuga menziesii</i> trunk mature	0.90 ± 0.09	-2.83 ± 0.12 (-3.13 –2.53)	0.99	< 0.0001	-5.05
<i>Taxodium distichum</i> branch, base of canopy	1.24 ± 0.10	-2.42 ± 0.07 (-2.57 –2.27)	0.95	< 0.0001	-4.02

PLC was derived from RWL by means of the “conifer-curve 1” [Eq. 4] presented in Fig. 2a. The parameter “ a ” corresponds to the slope of the linear part of the regression and “ b ” is the P_{50} , i.e., the pressure that is necessary to result in 50% conductivity loss. P_{88} is the pressure that would result in 88% conductivity loss. Results for a and P_{50} are given with \pm standard error, and the 95% confidence interval (CI 95%) is given in brackets. Information on the sample and dataset numbers is given in Table 1

Fig. 6 Predicted pressure application that is necessary to result in 50% conductivity loss (P_{50}) from the conifer-curve 1 [Eq. 4] related to P_{50} derived from experimental datasets. Detailed information on the predicted values can be found in Table 5. The gray dashed line indicates the 1:1 relationship



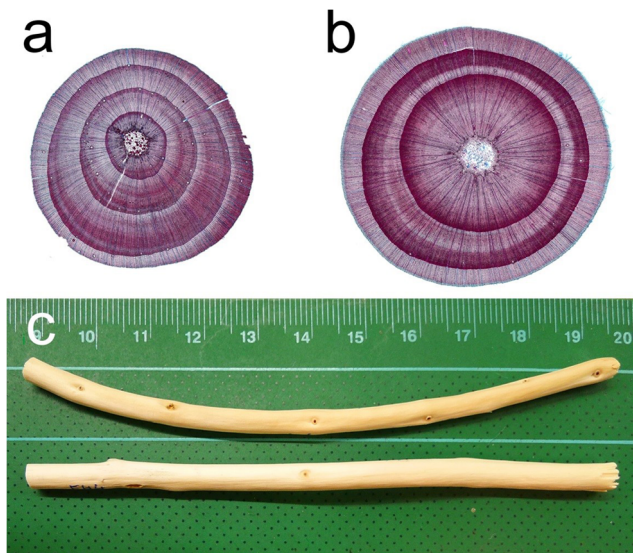


Fig. 7 Transverse sections of *Larix decidua* branch wood (a) and *Picea abies* young trunk wood (b). *L. decidua* contains compression wood that is common for conifers on the lower part of branches. Compression wood is characterized by higher density zones in the earlywood. Due to different shrinkage properties of wood differing in density, the *L. decidua* branch shows a concave bending at the compression wood side and a convex bending at the side of the opposite wood after drying at 103 °C (c, above), whereas it was straight at full saturation. The young trunk wood sample of a *P. abies* sapling remained straight after drying at 103 °C because the amount of late wood was quite consistent in each annual ring (c, below)

Open Access This article is distributed under the terms of the Creative Commons Attribution 4.0 International License (<http://creativecommons.org/licenses/by/4.0/>), which permits unrestricted use, distribution, and reproduction in any medium, provided you give appropriate credit to the original author(s) and the source, provide a link to the Creative Commons license, and indicate if changes were made.

References

- Allen CD, Breshears DD, McDowell NG (2015) On underestimation of global vulnerability to tree mortality and forest die-off from hotter drought in the Anthropocene. *Ecosphere* 6:129. <https://doi.org/10.1890/ES15-00203.1>
- Anfodillo T, Petit G, Crivellaro A (2013) Axial conduit widening in woody species: a still neglected anatomical pattern. *IAWA J* 34:352–364. <https://doi.org/10.1163/22941932-00000030>
- Barnard DM, Meinzer FC, Lachenbruch B, McCulloh KA, Johnson DM, Woodruff DR (2011) Climate-related trends in sapwood biophysical properties in two conifers: avoidance of hydraulic dysfunction through coordination adjustment in xylem efficiency, safety and capacitance. *Plant Cell Environ* 34:634–654. <https://doi.org/10.1111/j.1365-3040.2010.02269.x>
- Bertaud F, Holmbom B (2004) Chemical composition of earlywood and latewood in Norway spruce heartwood, sapwood and transition zone wood. *Wood Sci Technol* 38:245–256. <https://doi.org/10.1007/s00226-004-0241-9>
- Blackman CJ, Pfautsch S, Choat B, Delzon S, Gleason SM, Duursma RA (2016) Toward an index of desiccation time to tree mortality under drought. *Plant Cell Environ* 39:2342–2345. <https://doi.org/10.1111/pce.12758>
- Bouche PS, Larter M, Domec J-C, Burrell R, Gasson P, Jansen S, Delzon S (2014) A broad survey of hydraulic and mechanical safety in the xylem of conifers. *J Exp Bot* 65:4419–4431. <https://doi.org/10.1093/jxb/eru218>
- Braun HJ (1970) Funktionelle Histologie der sekundären Sprossachse: I. Das Holz. *Handbuch der Pflanzenanatomie IX/1*. Gebrüder Borntraeger, Berlin Stuttgart
- Choat B, Brodribb TJ, Brodersen CR, Duursma RA, Lopez R, Medlyn BE (2018) Triggers of tree mortality under drought. *Nature* 558:531–539. <https://doi.org/10.1038/s41586-018-0240-x>
- Choat B, Jansen S, Brodribb TJ, Cochard H, Delzon S, Bhaskar R, Bucci SJ, Feild TS, Gleason SM, Hacke UG, Jacobsen AL, Lens F, Maherali H, Martínez-Vilalta J, Mayr S, Mencuccini M, Mitchell PJ, Nardini A, Pitterman J, Pratt RB, Sperry JS, Westoby M, Wright IJ, Zanne AE (2012) Global convergence in the vulnerability of forests to drought. *Nature* 491:752–755. <https://doi.org/10.1038/nature11688>
- Cochard H, Lemoine D, Améglio T, Granier A (2001) Mechanisms of xylem recovery from winter embolism in *Fagus sylvatica*. *Tree Physiol* 21:27–33. <https://doi.org/10.1093/treephys/21.1.27>
- Cochard H, Badel E, Herbette S, Delzon S, Choat B, Jansen S (2013) Methods for measuring plant vulnerability to cavitation: a critical review. *J Exp Bot* 64:4779–4791. <https://doi.org/10.1093/jxb/ert193>
- Delzon S, Cochard H (2014) Recent advances in tree hydraulics highlight the ecological significance of the hydraulic safety margin. *New Phytol* 203:355–358. <https://doi.org/10.1111/nph.12798>
- Domec J-C, Gartner BL (2001) Cavitation and water storage in bole segments of mature and young Douglas-fir trees. *Trees* 15:204–214. <https://doi.org/10.1007/s004680100095>
- Domec J-C, Gartner BL (2002) Age- and position-related changes in hydraulic versus mechanical dysfunction of xylem: inferring the design criteria for Douglas-fir wood structure. *Tree Physiol* 22:91–104. <https://doi.org/10.1093/treephys/22.2-3.91>
- Domec J-C, Scholz FG, Bucci SJ, Meinzer FC, Goldstein G, Villalobos-Vega R (2006) Diurnal and seasonal variation in root xylem embolism in neotropical savanna woody species: impact on stomatal control of plant water status. *Plant Cell Environ* 29:26–35. <https://doi.org/10.1111/j.1365-3040.2005.01397.x>
- Domec J-C, Warren JM, Meinzer FC, Lachenbruch B (2009) Safety factors for xylem failure by implosion and air-seeding within roots, trunks and branches of young and old conifer trees. *IAWA J* 30:100–120. <https://doi.org/10.1163/22941932-90000207>
- Ennajeh M, Nouiri M, Khemira H, Cochard H (2011) Improvement to the air-injection technique to estimate xylem vulnerability to cavitation. *Trees Struct Funct* 25:705–710. <https://doi.org/10.1007/s00468-011-0548-8>
- Gleason SM, Blackman CJ, Cook AM, Laws CA, Westoby M (2014) Whole-plant capacitance, embolism resistance and slow transpiration rates all contribute to longer desiccation times in woody angiosperms from arid and wet habitats. *Tree Physiol* 34:275–284. <https://doi.org/10.1093/treephys/tpu001>
- Hacke UG, Lachenbruch B, Pitterman J, Mayr S, Domec J-C, Schulte PJ (2015) The hydraulic architecture of conifers. In: Hacke UG, ed. *Functional and ecological xylem anatomy*. Springer International Publishing Switzerland, 39–75
- Hacke UG, Sperry JS, Pockman WT, Davis SD, McCulloh KA (2001) Trends in wood density and structure are linked to prevention of xylem implosion by negative pressure. *Oecologia* 126:457–461. <https://doi.org/10.1007/s004420100628>
- Hammond WM, Yu KL, Wilson LA, Will RE, Anderegg WR, Adams HD (2019) Dead or dying? Quantifying the point of no return from hydraulic failure in drought-induced tree mortality. *New Phytol* (in press). <https://doi.org/10.1111/nph.15922>
- Hentschel R, Rosner S, Kayler ZE, Andreassen K, Børja I, Solberg S, Tveito OE, Priesack GA (2014) Norway spruce physiological and

- anatomical predisposition to dieback. For *Ecol Manag* 322:27–36. <https://doi.org/10.1016/j.foreco.2014.03.007>
- Hietz P, Rosner S, Sorz J, Mayr S (2008) Comparison of methods to quantify loss of hydraulic conductivity in Norway spruce. *Ann For Sci* 65:502–508. <https://doi.org/10.1051/forest.2008023>
- Holbrook NM (1995) Stem water storage. In: Gartner BL (ed) *Plant stem: physiology and functional morphology*. Academic Press, San Diego, pp 157–174
- IPCC (2013) Climate change 2013: the physical science basis. In: Stocker TF, Qin D, Plattner G-K, Tignor M, Allen SK, Boschung J, Nauels A, Xia Y, Bex V, Midgley PM (eds) *Contribution of working group I to the fifth assessment report of the intergovernmental panel on climate change*. Cambridge University press, Cambridge, New York, NY, p 1535
- IUCN (2019) The IUCN red list of threatened species. Version 2018-2. <http://www.iucnredlist.org>. Accessed 26 January 2019
- Johnson DM, McCulloh KA, Woodruff DR, Meinzer FC (2012) Hydraulic safety margins and embolism reversal in stems and leaves: why are conifers and angiosperms so different? *Plant Sci* 135:4–53. <https://doi.org/10.1016/j.plantsci.2012.06.010>
- Jupa R, Plavcová L, Gloser V, Jansen S (2016) Linking xylem water storage with anatomical parameters in five temperate tree species. *Tree Physiol* 36:756–769. <https://doi.org/10.1093/treephys/tpw020>
- Klein T, Zeppel MJ, Anderegg WR, Bloemen J, De Kauwe MG, Hudson P, Ruehr NK, Powell TL, von Arx G, Nardini A (2018) Xylem embolism refilling and resilience against drought-induced mortality in woody plants: processes and trade-offs. *Ecol Res* 33(5):839–855. <https://doi.org/10.1007/s11284-018-1588-y>
- Klein T, Cahanovitz R, Sprintsin M, Herr N, Schiller G (2019) A nationwide analysis of tree mortality under climate change: Forest loss and its causes in Israel 1948–2017. For *Ecol Manag* 432:840–849. <https://doi.org/10.1016/j.foreco.2018.10.020>
- Lachenbruch B, McCulloh KA (2014) Traits, properties, and performance: how woody plants combine hydraulic and mechanical functions in a cell, tissue, or whole plant. *New Phytol* 204:747–764. <https://doi.org/10.1111/nph.13035>
- Lopez OR, Kursar TA, Cochard H, Tyree MT (2005) Interspecific variation in xylem vulnerability to cavitation among tropical tree and shrub species. *Tree Physiol* 25:1553–1562. <https://doi.org/10.1111/j.1469-8137.2007.02235.x>
- Magnani F, Borghetti M (1995) Interpretation of seasonal changes of xylem embolism and plant hydraulic resistance in *Fagus sylvatica*. *Plant Cell Environ* 18:689–696. <https://doi.org/10.1111/j.1365-3040.1995.tb00570.x>
- Mayr S, Cochard H (2003) A new method for vulnerability analysis of small xylem areas reveals that compression wood of Norway spruce has lower hydraulic safety than opposite wood. *Plant Cell Environ* 26: 1365–1371. <https://doi.org/10.1046/j.0016-8025.2003.01060.x>
- Mayr S, Schmid P, Laur J, Rosner S, Charra-Vaskou K, Dämon B, Hacke UG (2014) Uptake of water via branches helps timberline conifers refill embolized xylem in late winter. *Plant Physiol* 164:1731–1740. <https://doi.org/10.1104/pp.114.236646>
- Mayr S, Rothart B, Wolfschwenger M (2006) Temporal and spatial pattern of embolism induced by pressure collar techniques in twigs of *Picea abies*. *J Exp Bot* 57:3157–3163. <https://doi.org/10.1093/jxb/erl077>
- McCulloh KA, Johnson DM, Meinzer FC, Woodruff DR (2014) The dynamic pipeline: hydraulic capacitance and xylem hydraulic safety in four tall conifer species. *Plant Cell Environ* 37:1171–1183. <https://doi.org/10.1111/pce.12225>
- McDowell NG, Allen CD (2015) Darcy's law predicts widespread forest mortality under climate warming. *Nat Clim Chang* 5:669–672. <https://doi.org/10.1038/nclimate2641>
- Meinzer FC, James SA, Goldstein G, Woodruff DR (2003) Whole-tree water transport scales with sapwood capacitance in tropical forest canopy trees. *Plant Cell Environ* 26:1147–1155. <https://doi.org/10.1046/j.1365-3040.2003.01039.x>
- Mencuccini M, Binks O (2015) Tall, leafy conifers lose out. *Nat Clim Chang* 5:625–626. <https://doi.org/10.1038/nclimate2698>
- Pivovarov AL, Burrell R, Lavigne B, Cochard H, Santiago LS, Delzon S (2016) Testing the 'microbubble effect' using the Cavitron technique to measure xylem water extraction curves. *AoB PLANTS* 8:plw011. <https://doi.org/10.1093/aobpla/plw011>
- Pammenter NW, VanderWilligen C (1998) A mathematical and statistical analysis of the curves illustrating vulnerability of xylem to cavitation. *Tree Physiol* 18:589–593. <https://doi.org/10.1093/treephys/18.8-9.589>
- Pratt RB, Jacobsen AL (2017) Conflicting demands on angiosperm xylem: tradeoffs among storage, transport and biomechanics. *Plant Cell Environ* 40:897–913. <https://doi.org/10.1111/pce.12862>
- Pratt RB, Jacobsen AL, Ewers FW, Davis SD (2007) Relationships among xylem transport, biomechanics and storage in stems and roots of nine *Rhamnaceae* species of the California chaparral. *New Phytol* 174:787–798. <https://doi.org/10.1111/j.1469-8137.2007.02061.x>
- Prendin AL, Mayr S, Beikircher B, von Arx G, Petit G (2018) Xylem anatomical adjustments prioritize hydraulic efficiency over safety as Norway spruce trees grow taller. *Tree Physiol* 38:1088–1097. <https://doi.org/10.1093/treephys/tpy065>
- Rosner S (2013) Hydraulic and biomechanical optimization in Norway spruce trunkwood: a review. *IAWA J* 34:365–390. <https://doi.org/10.1163/22941932-00000031>
- Rosner S (2017) Wood density as a proxy for vulnerability to cavitation: size matters. *J Plant Hydraulics* 4:e001. <https://doi.org/10.20870/jph.2017.e001>
- Rosner S, Gierlinger N, Klepsch M, Karlsson B, Evans R, Lundqvist S-O, Světlik J, Borja I, Dalsgaard L, Andreassen K, Solberg S, Jansen S (2018) Hydraulic and mechanical dysfunction of Norway spruce sapwood due to extreme summer drought in Scandinavia. For *Ecol Manag* 409:527–540. <https://doi.org/10.1016/j.foreco.2017.11.051>
- Rosner S, Heinze B, Savi T, Dalla-Salda G (2019) Prediction of hydraulic conductivity loss from relative water loss: new insights into water storage of tree stems and branches. *Physiol Plant* 165:843–854. <https://doi.org/10.1111/ppl.12790>
- Rosner S, Klein A, Müller U, Karlsson B (2008) Tradeoffs between hydraulic and mechanical stress response of mature Norway spruce trunkwood. *Tree Physiol* 28:1179–1188. <https://doi.org/10.1093/treephys/28.8.1179>
- Savi T, Love VL, Dal Borgo A, Martellos S, Nardini A (2017) Morpho-anatomical and physiological traits in saplings of drought-tolerant Mediterranean woody species. *Trees* 31:1137–1148. <https://doi.org/10.1007/s00468-017-1533-7>
- Savi T, Tintner J, Da Sois L, Grabner M, Petit G, Rosner S (2019) The potential of mid-infrared spectroscopy for prediction of wood density and vulnerability to embolism in woody angiosperms. *Tree Physiol* (in press). <https://doi.org/10.1093/treephys/tpy112>
- Scholz FG, Bucci SJ, Goldstein G, Meinzer FC, Franco AC, Miralles-Wilhelm F (2007) Biophysical properties and functional significance of stem water storage tissues in neotropical savanna trees. *Plant Cell Environ* 30:236–248. <https://doi.org/10.1111/j.1365-3040.2006.01623.x>
- David-Schwartz R, Paudel I, Mizrahi M, Delzon S, Cochard H, Lukyanov V, Badel E, Capdeville G, Shklar G, Cohen S (2016) Indirect evidence for genetic differentiation in vulnerability to embolism in *Pinus halepensis*. *Front Plant Sci* 7:768. <https://doi.org/10.3389/fpls.2016.00768>
- Schweingruber FH, Bömer A, Schulze E-D (2008) *Atlas of woody plant stems: evolution, structure and environmental modifications*. Springer-Verlag, Berlin Heidelberg

- Solberg S (2004) Summer drought: a driver for crown condition and mortality of Norway spruce in Norway. *Forest Pathol* 34:93–104. <https://doi.org/10.1111/j.1439-0329.2004.00351.x>
- Sperry JS, Tyree MT (1988) Mechanism of water stress-induced xylem embolism. *Plant Physiol* 88:581–587
- Spicer R, Gartner BL (1998) Hydraulic properties of Douglas-fir (*Pseudotsuga menziesii*) branches and branch halves with references to compression wood. *Tree Physiol* 18:777–784. <https://doi.org/10.1093/treephys/18.11.777>
- Trifilò P, Nardini A, Lo Gullo MA, Barbera PM, Savi T, Raimondo F (2015) Diurnal changes in embolism rate in nine dry forest trees: relationships with species-specific xylem vulnerability, hydraulic strategy and wood traits. *Tree Physiol* 35:694–705. <https://doi.org/10.1093/treephys/tpv049>
- Tyree MT, Yang S (1990) Water-storage capacity of Thuja, Tsuga and Acer stems measured by dehydration isotherms. *Planta* 182:420–426. <https://doi.org/10.1007/BF02411394>
- Tyree MT, Sperry JS (1988) Do woody plants operate near the point of catastrophic xylem dysfunction caused by dynamic water stress? Answers from a model. *Plant Physiol* 88:574–580
- Voltas J, Shestakova TA, Patsiou T, Di Matteo G, Klein T (2018) Ecotypic variation and stability in growth performance of the thermophilic conifer *Pinus halepensis* across the Mediterranean basin. *Forest Ecol Managem* 424:205–215. <https://doi.org/10.1016/j.foreco.2018.04.058>

Publisher's note Springer Nature remains neutral with regard to jurisdictional claims in published maps and institutional affiliations.